Iterative Reconstructions
State of the Art & Optimisations

EPU - Traitement d'images en Physique Médicale
Port Bourgenay

Benoit Recur
INSERM U-1029 - Noctylio S.A.S

7-9 Octobre 2015

Outline

Introduction to tomography

- **Processing sequence**;
- **Computed tomography**.

Introduction to Iterative Reconstruction

- **Examples**;
- **Algebraic reconstruction technique (ART)**;
- **Convergence**.

From definitions of acquisition properties ...

- **Projection matrix**;
- **Forward model**;
- **A priori on solution**.

... to statistical methods

- **for emission tomography**;
- **for transmission tomography**.

Towards application based optimisations

- **Some examples**;
- **Concept of full iterative techniques (co-design)**.

Outline

Introduction to tomography

- **Processing sequence;**
- **Computed tomography.**

Introduction to Iterative Reconstruction

- **Examples;**
- **Algebraic reconstruction technique (ART);**
- **Convergence.**

From definitions of acquisition properties ...

- **Projection matrix;**
- **Forward model;**
- **A priori on solution.**

... to statistical methods

- **for emission tomography;**
- **for transmission tomography.**

Towards application based optimisations

- **Some examples;**
- **Concept of full iterative techniques (co-design).**

Imaging Processing Sequence

Imaging Processing Sequence

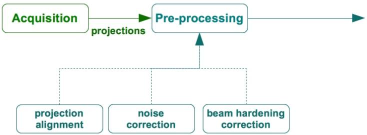

Imaging Processing Sequence

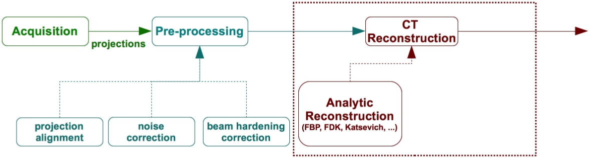

Imaging Processing Sequence

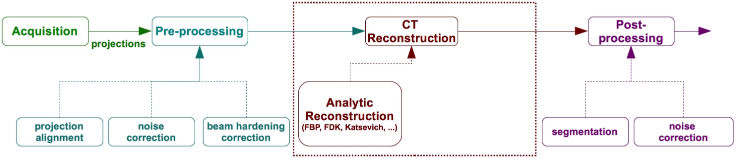

Imaging Processing Sequence

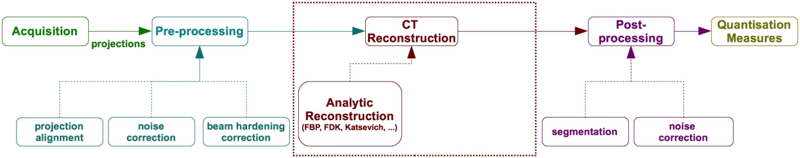

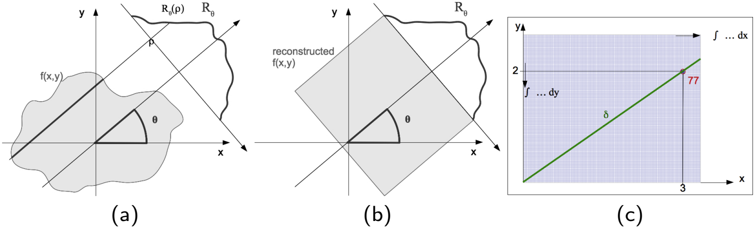

Figure: (a) Projection line defined by angle θ and position ρ. Its value is the integral of $f(x, y)$ along the line (θ, ρ). (b) Data acquired on one projection are not enough to recover the acquired space. (c) Example of 2D acquisition along the line restricted by a Dirac pulse.

Direct Transform

$$\mathcal{R}_\theta(\rho) = \int_{-\infty}^{\infty} \int_{-\infty}^{\infty} f(x, y)\delta(\rho - x\cos\theta - y\sin\theta)dxdy \tag{1}$$

Computed Tomography

Radon Transform

- Principle of tomodensitometry: measure X-Ray attenuation;
- Radon transform ⇔ projection ⇔ radiography;
- Sinogram = projection set.

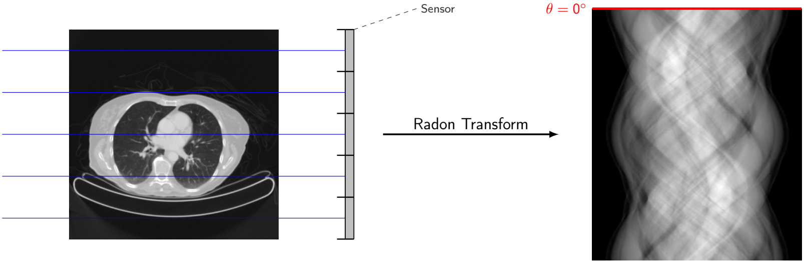

Images: H. Der Sarkissian PhD Thesis (2015).

Computed Tomography

Radon Transform

- Principle of tomodensitometry: measure X-Ray attenuation;
- Radon transform $\Leftrightarrow$ projection $\Leftrightarrow$ radiography;
- Sinogram = projection set.

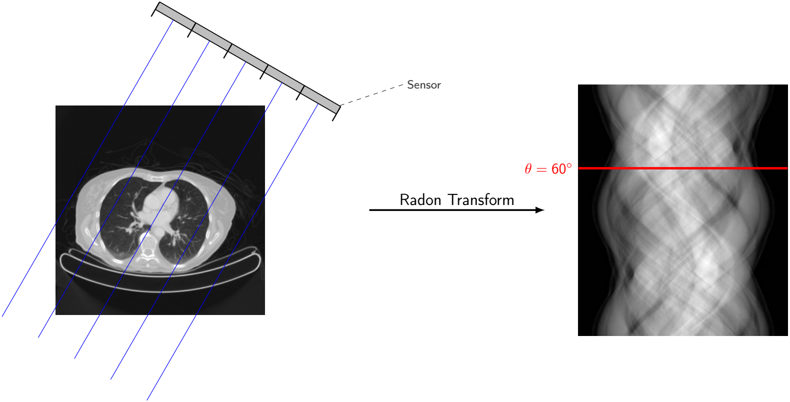

Images: H. Der Sarkissian PhD Thesis (2015).

Computed Tomography

Radon Transform

- Principle of tomodensitometry: measure X-Ray attenuation;
- Radon transform ⇔ projection ⇔ radiography;
- Sinogram = projection set.

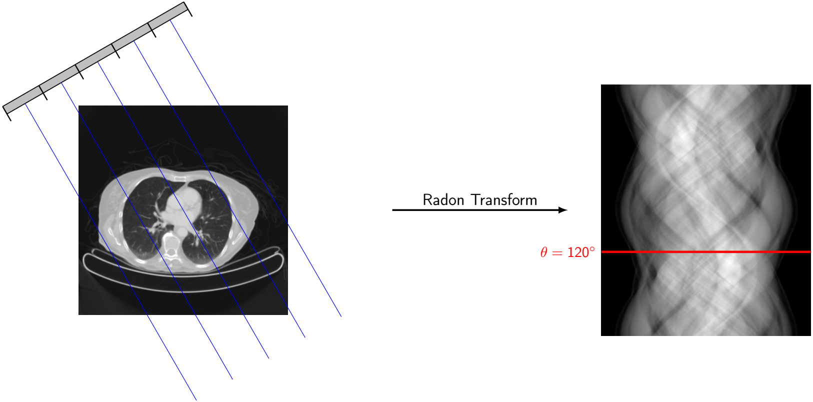

Images: H. Der Sarkissian PhD Thesis (2015).

Computed Tomography
Radon Transform

- Principle of tomodensitometry: measure X-Ray attenuation;
- Radon transform ⇔ projection ⇔ radiography;
- Sinogram = projection set.

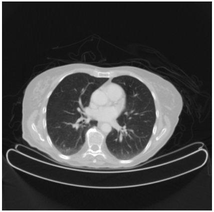

Reconstructed Slice

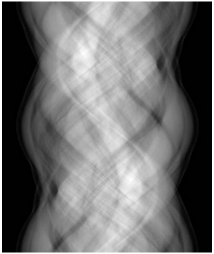

Measured Sinogram

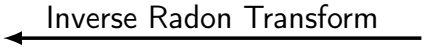

Images: H. Der Sarkissian PhD Thesis (2015).

Computed Tomography

Reconstruction (FBP-like)

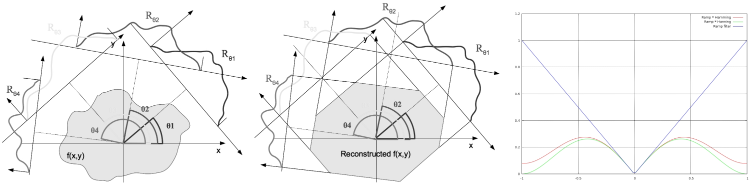

(a) (b) (c)

Figure: (a) Acquisition on several viewing angles. (b) Intersecting data contained on the projection set leads to a better estimation of the acquired space f. (c) Example of some ramp-filters.

Filtered Back-Projection

$$f(x,y) = \int_0^{\pi} \int_{-\infty}^{\infty} \mathcal{W}_\theta(\rho)\delta(\rho - x\cos\theta - y\sin\theta)d\rho d\theta \qquad (2)$$

Where :

$$\mathcal{W}_\theta(\rho) = \int_{-\infty}^{\infty} |\nu| \left(\int_{-\infty}^{\infty} \mathcal{R}_\theta(\rho_s)e^{-i2\pi\rho_s\nu}d\rho_s \right) e^{i2\pi\rho\nu}d\nu \qquad (3)$$

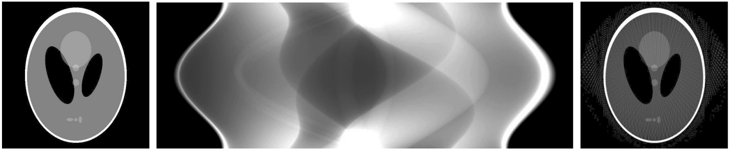

(a) (b) (c)

Figure: (a) Image acquired with $N_\theta = 180$ projections. (b) Sinogram. Lines: projection for each viewing angle (uniformly distributed between 0 et π). Columns: projection value (sum of crossed pixels) at each position ρ. (c) Image reconstructed from the sinogram using FBP.

Computed Tomography

Limitations of analytic methods

- Defined in continuous space with parallel beam;
- Discretisation implies:
  - very sensitive to projection number (Nyquist);
  - Parallel beam only (except some specific implementations as FDK / Katsevich);
  - Not compatible with emission tomography (geometrical limitations due to viewing angle of each collimated sensor);
- Physics of radiation not modelled;
- Noise distribution neglected.

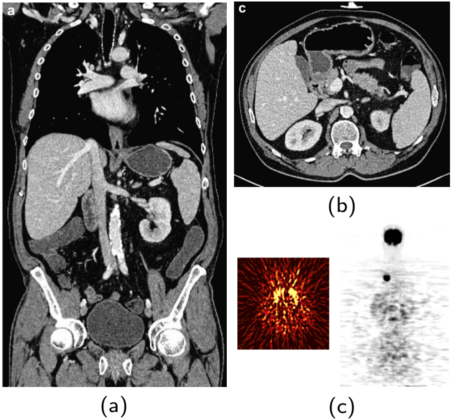

Figure: (a-b) FBP reconstruction (transversal / coronal, resp.) from X-Ray CT acquisition. (c) FBP reconstructions from SPECT acquisitions.

Images from: Physica Medica 28, 94-108 (2012).

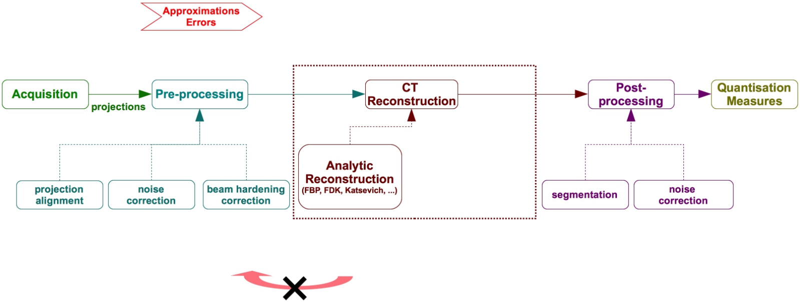

Approximations
Errors
Acquisition
projections
Pre-processing
CT
Reconstruction
Post-
processing
Quantisation
Measures
projection
alignment
noise
correction
beam hardening
correction
Analytic
Reconstruction
(FBP, FDK, Katsevich, ...)
segmentation
noise
correction

Outline

Introduction to tomography

- **Processing sequence**;
- **Computed tomography**.

Introduction to Iterative Reconstruction

- **Examples**;
- **Algebraic reconstruction technique (ART)**;
- **Convergence**.

From definitions of acquisition properties ...

- **Projection matrix**;
- **Forward model**;
- **A priori on solution**.

... to statistical methods

- **for emission tomography**;
- **for transmission tomography**.

Towards application based optimisations

- **Some examples**;
- **Concept of full iterative techniques (co-design)**.

Towards Iterative Reconstructions

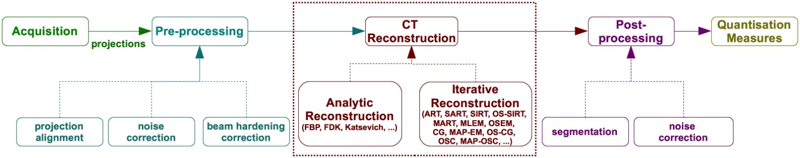

Towards Iterative Reconstructions

- Algebraic Reconstruction Techniques (ART):
  Simultaneous-ART, Simultaneous Iterative Reconstruction Technique (SIRT), Ordered Subset (OS-)SIRT, Adaptive ART, Multiplicative ART, ...
- Bayesian Techniques:
  Expectation Maximisation (EM), OS-EM, Maximum A Posteriori (MAP-)EM, Maximum Likelihood for transmission tomography (ML-TR), Ordered Subset Convex methods (OSC), ...
- Gradient Methods:
  Conjugate Gradient (CG), OS-CG, Coordinate CG (CCG), ...

Towards Iterative Reconstructions

- Algebraic Reconstruction Techniques (ART):
  Simultaneous-ART, Simultaneous Iterative Reconstruction Technique (SIRT), Ordered Subset (OS-)SIRT, Adaptive ART, Multiplicative ART, ...
- Bayesian Techniques:
  Expectation Maximisation (EM), OS-EM, Maximum A Posteriori (MAP-)EM, Maximum Likelihood for transmission tomography (ML-TR), Ordered Subset Convex methods (OSC), ...
- Gradient Methods:
  Conjugate Gradient (CG), OS-CG, Coordinate CG (CCG), ...

A Wide range of methods

- To address different implementation limitations;
- To deal with the ill-posed problem and noise;
- To optimise convergence of the solution;
- and just for the pleasure to make everybody crazy !

Towards Iterative Reconstructions

- Algebraic Reconstruction Techniques (ART):
  Simultaneous-ART, Simultaneous Iterative Reconstruction Technique (SIRT), Ordered Subset (OS-)SIRT, Adaptive ART, Multiplicative ART, ...
- Bayesian Techniques:
  Expectation Maximisation (EM), OS-EM, Maximum A Posteriori (MAP-)EM, Maximum Likelihood for transmission tomography (ML-TR), Ordered Subset Convex methods (OSC), ...
- Gradient Methods:
  Conjugate Gradient (CG), OS-CG, Coordinate CG (CCG), ...

A Wide range of methods

- To address different implementation limitations;
- To deal with the ill-posed problem and noise;
- To optimise convergence of the solution;
- and just for the pleasure to make everybody crazy !

Even if, practically, some iterative methods (and their implementation) outperform other iterative techniques, they are theoretically similar. Every **optimizations** of iterative CT reconstructions could be done with any of them !

Iterative Reconstruction

"A bit of Maths"

$p(R|\mu)$, expectation to observe measurements R of a given sample μ:

$$p(R|\mu) = \textbf{Poisson}\left\{\underbrace{I_0(i)\mathrm{e}^{-\sum_j w_{ij}\mu(j)}}_{\hat{R}(i)} + bg(i)\right\} \text{ where } \begin{cases} i\text{: projection line index,} \\ \hat{R}\text{: expected photon counts at } i, \\ I_0\text{: maximal photon counts,} \\ bg\text{: background noise,} \\ w_{ij}\text{: voxel } j \text{ contribution on } i. \end{cases} \quad (4)$$

Penalization term $p(\mu)$ to regularize the solution:

$$p(\mu) = e^{-\sum_j \sum_{k\in\mathcal{N}(j)} y_{jk}\Phi(\mu(j)-\mu(k))} \text{ where } \begin{cases} \mathcal{N}(j)\text{: neighbourhood of pixel } j, \\ \Phi(\cdot)\text{: potential function,} \\ y_{jk}\text{: weight factor.} \end{cases} \quad (5)$$

$$\Phi(x) = 2\gamma t^2 \log\cosh\left(\frac{|x|}{t}\right), \text{ where } t\text{: threshold, } \gamma\text{: sensitivity parameter.} \quad (6)$$

Maximizing $L = \log\left[p(R|\mu)p(\mu)\right]$ (Newton-Raphson):

$$\mu_{s+1}^t(j) = \mu_s^t(j) + \underbrace{\Delta\mu_s^t(j)}_{-\frac{\partial L}{\partial^2 L}}, \Delta\mu_s^t(j) = \frac{\sum_{i\in S(s)} w_{ij}\left[\hat{R}_s^t(i) - R(i)\right] - \sum_{k\in\mathcal{N}(j)} y_{jk}\Phi'\left[\mu_s^t(j)-\mu_s^t(k)\right]}{\sum_{i\in S(s)} w_{ij}\left(\sum_l w_{il}\right)\hat{R}_s^t(i) + \sum_{k\in\mathcal{N}(j)} y_{jk}\Phi''\left[\mu_s^t(j)-\mu_s^t(k)\right]} \quad (7)$$

Iterative Reconstruction

"is a game !"

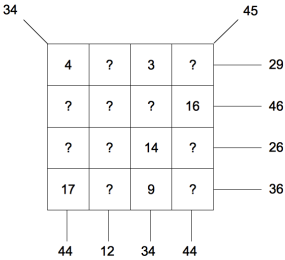

Figure: Magic square to recover from sums along lines, columns et diagonals.

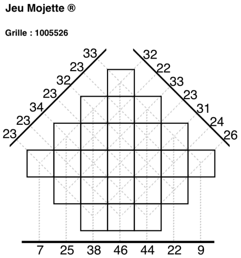

Figure: Mojette game: projections and *a priori* on the solution (3 different pixel values only).

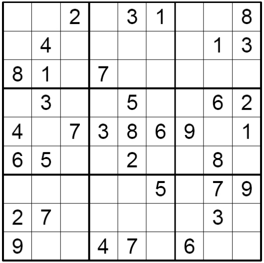

Figure: Sudoku (hidden projection values), and lots of *a priori* about the solution.

Iterative Reconstruction

"is a game !"

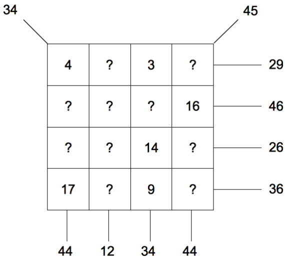

Figure: Magic square to recover from sums along lines, columns et diagonals.

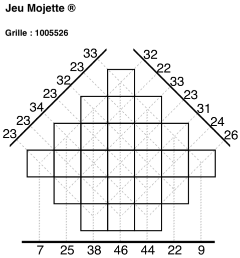

Figure: Mojette game: projections and *a priori* on the solution (3 different pixel values only).

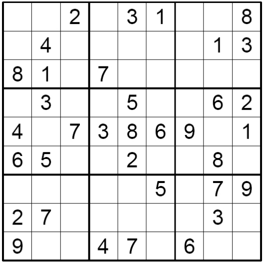

Figure: Sudoku (hidden projection values), and lots of *a priori* about the solution.

In these games: a priori and pre-conditioning on the solution lead to unique solution.

Iterative Reconstruction

Example

4	2
1	11

Images: H. Der Sarkissian (2015).

Iterative Reconstruction

Example

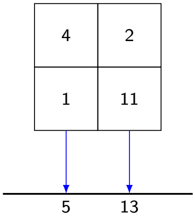

Images: H. Der Sarkissian (2015).

Iterative Reconstruction

Example

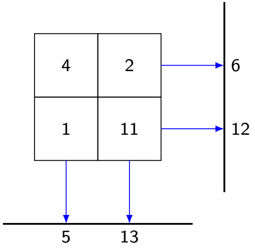

Images: H. Der Sarkissian (2015).

Iterative Reconstruction

Example

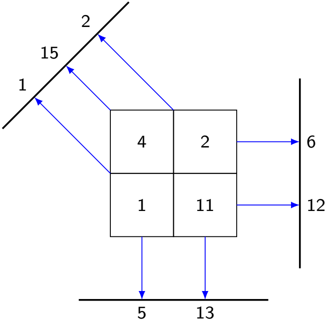

Images: H. Der Sarkissian (2015).

Iterative Reconstruction
Example

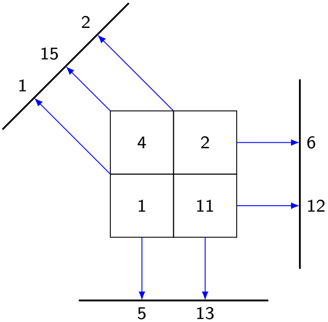

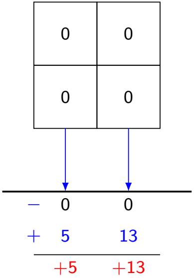

Images: H. Der Sarkissian (2015).

Iterative Reconstruction

Example

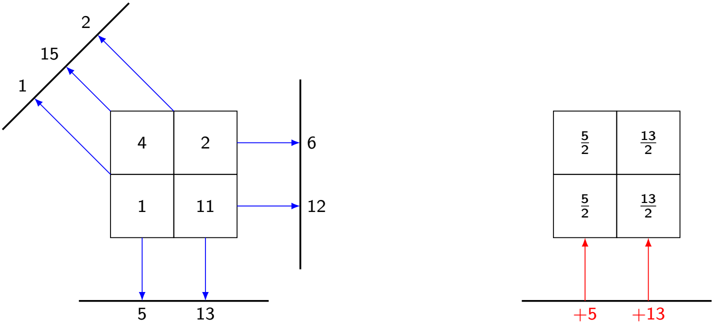

Images: H. Der Sarkissian (2015).

Iterative Reconstruction

Example

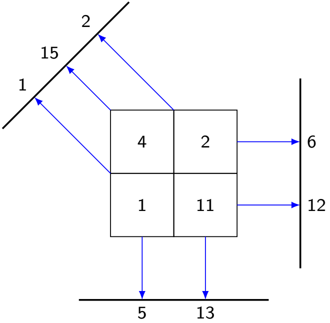

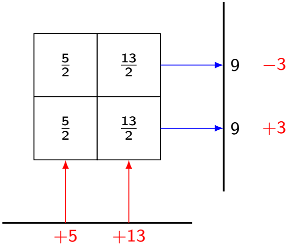

Images: H. Der Sarkissian (2015).

Iterative Reconstruction

Example

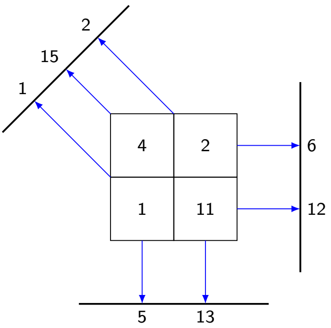

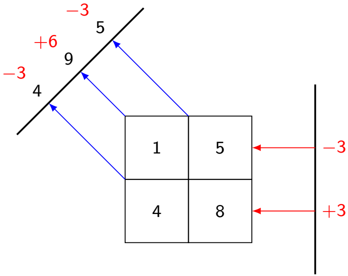

Images: H. Der Sarkissian (2015).

Iterative Reconstruction

Example

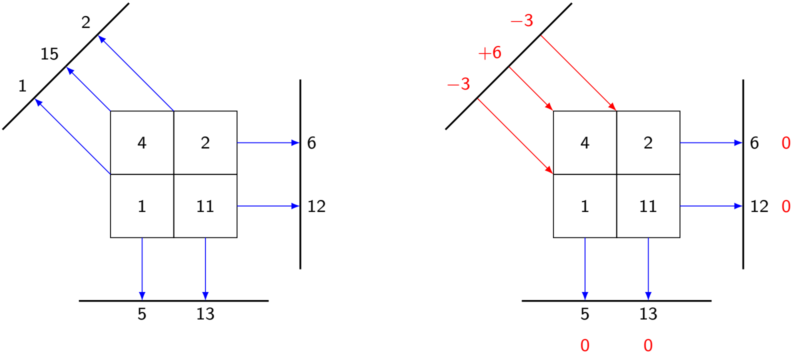

Images: H. Der Sarkissian (2015).

Solve $B = R.I$ where:

- $B = (b_{\mathbf{1}}, b_{\mathbf{2}}, \ldots, b_i, \ldots, b_M)^T$: acquisition;
- $I = (p_{\mathbf{1}}, p_{\mathbf{2}}, \ldots, p_j, \ldots, p_N)^T$: image to reconstruct;
- $R = \{w_{ij}\}, i \in [1, M] \wedge j \in [1, N]$: acquisition matrix sized $M \times N$.

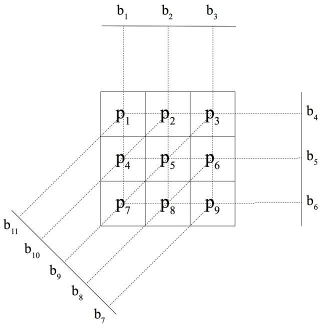

$$
\begin{cases}
b_{\mathbf{1}} = p_{\mathbf{1}} + p_{\mathbf{4}} + p_{\mathbf{7}} \\
b_{\mathbf{2}} = p_{\mathbf{2}} + p_{\mathbf{5}} + p_{\mathbf{8}} \\
b_{\mathbf{3}} = p_{\mathbf{3}} + p_{\mathbf{6}} + p_{\mathbf{9}} \\
b_{\mathbf{4}} = p_{\mathbf{1}} + p_{\mathbf{2}} + p_{\mathbf{3}} \\
b_{\mathbf{5}} = p_{\mathbf{4}} + p_{\mathbf{5}} + p_{\mathbf{6}} \\
b_{\mathbf{6}} = p_{\mathbf{7}} + p_{\mathbf{8}} + p_{\mathbf{9}} \\
\quad \ldots \\
b_i = \sum_j w_{ij} p_j \\
\quad \ldots
\end{cases}
$$

Iterative Reconstruction

Example

Solve $B = R.I$ where:

- $B = (b_1, b_2, \ldots, b_i, \ldots, b_M)^T$: acquisition;
- $I = (p_1, p_2, \ldots, p_j, \ldots, p_N)^T$: image to reconstruct;
- $R = \{w_{ij}\}, i \in [1, M] \wedge j \in [1, N]$: acquisition matrix sized $M \times N$.

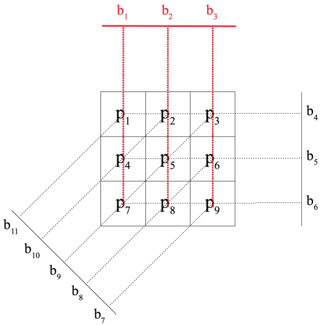

$$\begin{cases} b_1 = p_1 + p_4 + p_7 \\ b_2 = p_2 + p_5 + p_8 \\ b_3 = p_3 + p_6 + p_9 \\ b_4 = p_1 + p_2 + p_3 \\ b_5 = p_4 + p_5 + p_6 \\ b_6 = p_7 + p_8 + p_9 \\ \ldots \\ b_i = \sum_j w_{ij} p_j \\ \ldots \end{cases}$$

$$\begin{cases} b_1^1 = p_1^1 + p_4^1 + p_7^1 \\ b_2^1 = p_2^1 + p_5^1 + p_8^1 \\ b_3^1 = p_3^1 + p_6^1 + p_9^1 \end{cases}$$

$$\begin{cases} \Delta p_1^2 = b_1 - b_1^1/3 \\ \Delta p_4^2 = b_1 - b_1^1/3 \\ \Delta p_7^2 = b_1 - b_1^1/3 \\ \Delta p_2^2 = b_2 - b_2^1/3 \\ \ldots \end{cases}$$

Iterative Reconstruction

Example

Solve $B = R.I$ where:

- $B = (b_1, b_2, \dots, b_i, \dots, b_M)^T$: acquisition;
- $I = (p_1, p_2, \dots, p_j, \dots, p_N)^T$: image to reconstruct;
- $R = \{w_{ij}\}, i \in [1, M] \wedge j \in [1, N]$: acquisition matrix sized $M \times N$.

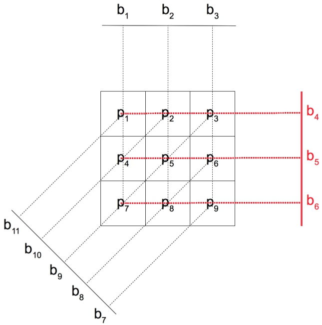

$$
\begin{cases}
b_1 = p_1 + p_4 + p_7 \\
b_2 = p_2 + p_5 + p_8 \\
b_3 = p_3 + p_6 + p_9 \\
b_4 = p_1 + p_2 + p_3 \\
b_5 = p_4 + p_5 + p_6 \\
b_6 = p_7 + p_8 + p_9 \\
\dots \\
b_i = \sum_j w_{ij} p_j \\
\dots
\end{cases}
$$

$$
\begin{cases}
b_4^{k,s} = p_1^{k,s-1} + p_2^{k,s-1} + p_3^{k,s-1} \\
b_5^{k,s} = \sum_j w_{5j} p_j^{k,s-1} \\
\dots
\end{cases}
$$

$$
\begin{cases}
p_j^{k,s} = p_j^{k,s-1} + \dfrac{b_i - b^{k,s}}{\sum_j w_{ij} = ||b_i||} \\
\dots
\end{cases}
$$

Iterative Reconstruction

Example

Algebraic Reconstruction Techniques

- ART: update at each projection line i:

$$p_j^{k,s} = p_j^{k,s-\mathbf{1}} + \lambda w_{ij} \frac{b_i - b_i^{k,s}}{||b_i||}$$

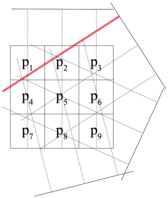

ART

Algebraic Reconstruction Techniques

- ART: update at each projection line i:

$$p_j^{k,s} = p_j^{k,s-\mathbf{1}} + \lambda w_{ij} \frac{b_i - b_i^{k,s}}{||b_i||}$$

- SART: update at each projection (all i in θ-projection);
- OS-SIRT: update at each projection subset ;
- SIRT: update from all projections.

$$p_j^{k,s} = p_j^{k,s-\mathbf{1}} + \lambda \frac{\sum_i w_{ij} \frac{b_i - b_i^{k,s}}{||b_i||}}{\sum_i w_{ij}}$$

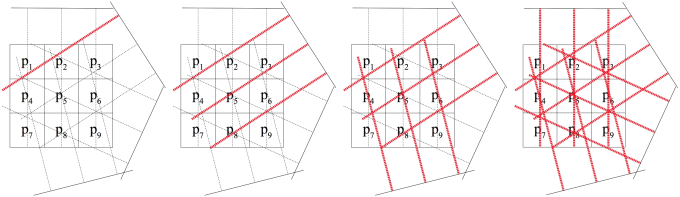

ART **SART** **OS-SIRT** **SIRT**

Iterative Reconstruction

Example

Algebraic Reconstruction Techniques

- ART: update at each projection line i:

- SART: update at each projection (all i in θ-projection);
- OS-SIRT: update at each projection subset ;
- SIRT: update from all projections.

$$p_j^{k,s} = p_j^{k,s-1} + \lambda w_{ij} \frac{b_i - b_i^{k,s}}{||b_i||}$$

$$p_j^{k,s} = p_j^{k,s-1} + \lambda \frac{\sum_i w_{ij} \frac{b_i - b_i^{k,s}}{||b_i||}}{\sum_i w_{ij}}$$

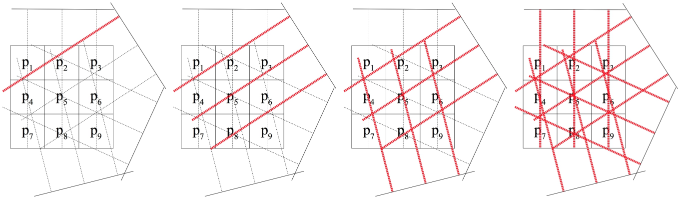

ART **SART** **OS-SIRT** **SIRT**

Iterative Reconstruction in the processing sequence

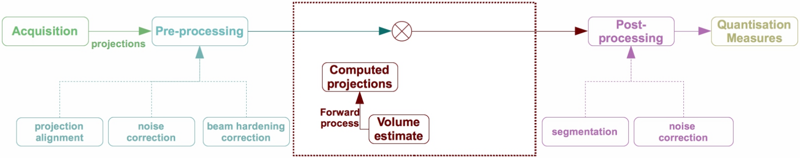

Iterative Reconstruction in the processing sequence

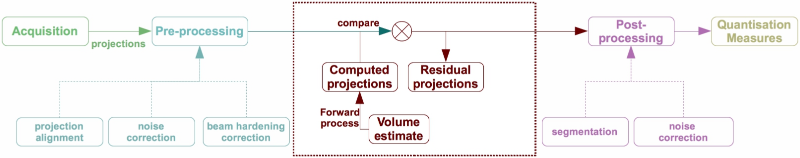

Iterative Reconstruction in the processing sequence

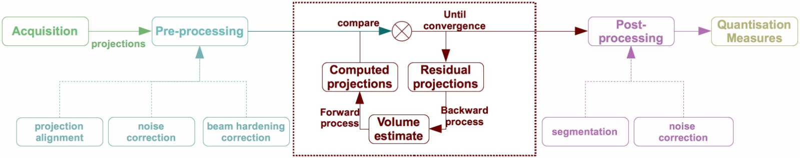

Iterative Reconstruction needs to deal with:

Acquisition properties

- How to define the projection matrix A (acquisition geometry);
- Forward model including appropriate physics of radiation;
- Incorporate *a priori* on solution / noise distribution, motion correction, ...

Convergence

- What the better first estimate ?;
- Ordered subsets of projections;
- How to detect it and avoid divergence;

Iterative Reconstruction needs to deal with:

Acquisition properties

- How to define the projection matrix A (acquisition geometry);
- Forward model including appropriate physics of radiation;
- Incorporate *a priori* on solution / noise distribution, motion correction, ...

Convergence

- What the better first estimate ?;
- Ordered subsets of projections;
- How to detect it and avoid divergence;

Iterative Reconstruction needs to deal with: Convergence

What is the better first estimate ?

Iterative Reconstruction needs to deal with: Convergence

What is the better first estimate ?

- empty or uniform image;
- FBP-like reconstruction.

Iterative Reconstruction needs to deal with: Convergence

What is the better first estimate ?

- empty or uniform image;
- FBP-like reconstruction.

How to detect convergence ?

- Define number of super-iterations:

Iterative Reconstruction needs to deal with: Convergence

What is the better first estimate ?

- empty or uniform image;
- FBP-like reconstruction.

How to detect convergence ?

- Define number of super-iterations:
  - Best convergence not assumed;
  - Divergence not detected;

Iterative Reconstruction needs to deal with: Convergence

What is the better first estimate ?

- empty or uniform image;
- FBP-like reconstruction.

How to detect convergence ?

- Define number of super-iterations:
  - Best convergence not assumed;
  - Divergence not detected;
- Follow the error during iterations and break if it starts to increase:

Iterative Reconstruction needs to deal with: Convergence

What is the better first estimate ?

- empty or uniform image;
- FBP-like reconstruction.

How to detect convergence ?

- Define number of super-iterations:
  - Best convergence not assumed;
  - Divergence not detected;
- Follow the error during iterations and break if it starts to increase:
  - error increases $\neq$ divergence starts;

Iterative Reconstruction needs to deal with: Convergence

What is the better first estimate ?

- empty or uniform image;
- FBP-like reconstruction.

How to detect convergence ?

- Define number of super-iterations:
  - Best convergence not assumed;
  - Divergence not detected;
- Follow the error during iterations and break if it starts to increase:
  - error increases $\neq$ divergence starts;
- Threshold on the error back-projected into volume during update:

Iterative Reconstruction needs to deal with: Convergence

What is the better first estimate ?

- empty or uniform image;
- FBP-like reconstruction.

How to detect convergence ?

- Define number of super-iterations:
  - Best convergence not assumed;
  - Divergence not detected;
- Follow the error during iterations and break if it starts to increase:
  - error increases $\neq$ divergence starts;
- Threshold on the error back-projected into volume during update:
  - may be never reached;

Iterative Reconstruction needs to deal with: Convergence

What is the better first estimate ?

- empty or uniform image;
- FBP-like reconstruction.

How to detect convergence ?

- Define number of super-iterations:
  - Best convergence not assumed;
  - Divergence not detected;
- Follow the error during iterations and break if it starts to increase:
  - error increases $\neq$ divergence starts;
- Threshold on the error back-projected into volume during update:
  - may be never reached;
- Combine previous ones + regularise the solution:

Iterative Reconstruction needs to deal with: Convergence

What is the better first estimate ?

- empty or uniform image;
- FBP-like reconstruction.

How to detect convergence ?

- Define number of super-iterations:
  - Best convergence not assumed;
  - Divergence not detected;
- Follow the error during iterations and break if it starts to increase:
  - error increases $\neq$ divergence starts;
- Threshold on the error back-projected into volume during update:
  - may be never reached;
- Combine previous ones + regularise the solution:
  - implies rigorous parameterisations of breaking conditions and regularisation.

Iterative Reconstruction needs to deal with: Convergence

Ordered subsets of projections

- **Ordered projections (SART context):**

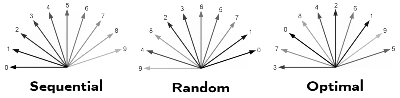

Figure: From darkest to lightest: sequence of projection/backprojection updates.

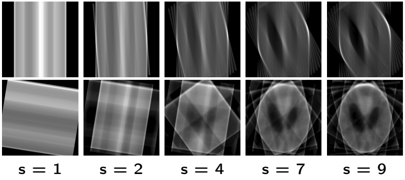

Figure: Reconstruction according to projection numbers and orientations.

Iterative Reconstruction needs to deal with: Convergence

Ordered subsets of projections

- Ordered projections (SART context):

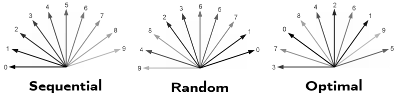

Figure: From darkest to lightest: sequence of projection/backprojection updates.

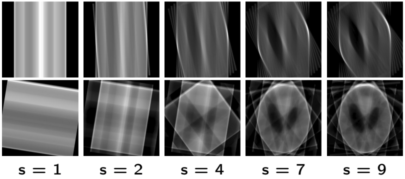

Figure: Reconstruction according to projection numbers and orientations.

- Ordered Subsets of projections (OS context):

$$\{0, \frac{\pi}{8}, \frac{\pi}{4}, \frac{3\pi}{8}, \frac{\pi}{2}, \frac{5\pi}{8}, \frac{3\pi}{4}, \frac{7\pi}{8}\} \Leftrightarrow \{0, \frac{\pi}{2}\} \wedge \{\frac{\pi}{4}, \frac{3\pi}{4}\} \wedge \{\frac{\pi}{8}, \frac{5\pi}{8}\} \wedge \{\frac{3\pi}{8}, \frac{7\pi}{8}\}$$

  - all projections in a subset having the lowest inter-correlation;
  - each subsequent subset is the lowest correlated to the previous ones.

Outline

Introduction to tomography

- **Processing sequence;**
- **Computed tomography.**

Introduction to Iterative Reconstruction

- **Examples;**
- **Algebraic reconstruction technique (ART);**
- **Convergence.**

From definitions of acquisition properties ...

- **Projection matrix;**
- **Forward model;**
- **A priori on solution.**

... to statistical methods

- **for emission tomography;**
- **for transmission tomography.**

Towards application based optimisations

- **Some examples;**
- **Concept of full iterative techniques (co-design).**

- How to define the projection matrix A (acquisition geometry);
- Forward model including appropriate physics of radiation;
- Incorporate *a priori* on solution / noise distribution, motion correction, ...

Acquisition properties

How to define the acquisition geometry (matrix A)

X-Ray CT scanner geometry

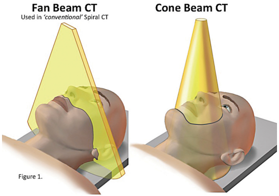

image from: http://www.oralhealthgroup.com/

- Parallel beam:
  - Theoretical geometry (Radon);
  - Industrial tomographs;
  - rebinning other geometries;
- Fan-beam:
  - set of 1D projections by slice;
  - spiral source trajectory;
- Cone-Beam
  - set of 2D projections;
  - spiral / helical source trajectory;

Acquisition properties

How to define the acquisition geometry (matrix A)

X-Ray CT scanner geometry

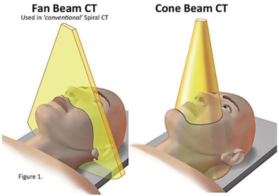

image from: http://www.oralhealthgroup.com/

- Parallel beam:
  - Theoretical geometry (Radon);
  - Industrial tomographs;
  - rebinning other geometries;
- Fan-beam:
  - set of 1D projections by slice;
  - spiral source trajectory;
- Cone-Beam
  - set of 2D projections;
  - spiral / helical source trajectory;

Parallel-beam

Fan-beam (spiral), angle $\approx 30^\circ$.

CB, angle $\approx 30^\circ$, 64 rows.

Acquisition properties

How to define the acquisition geometry (matrix A)

X-Ray CT scanner geometry:

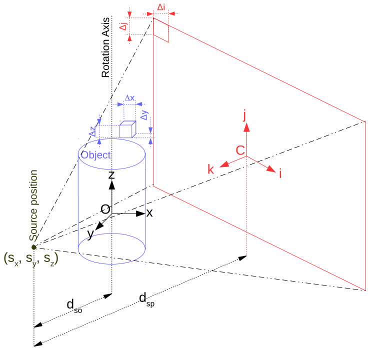

- $(\Delta x, \Delta y, \Delta z)$: voxel dimension;
- $(\Delta i, \Delta j)$: projection pixel dimension;
- (s_x, s_y, s_z): source position for projection θ;
- (c_x, c_y, c_z): panel center position of projection θ;
- d_{SO}: distance source $S \leftrightarrow$ rotation axis;
- d_{SP}: distance source $S \leftrightarrow$ panel center C;
- pitch: Z-translation (helical scanning);
- panel curvature;
- $W \times H \times D$: reconstructed volume size (in voxels);
- $I \times J$: panel size (in pixels);
- ...

Acquisition properties

How to define the acquisition geometry (matrix A)

X-Ray CT scanner geometry:

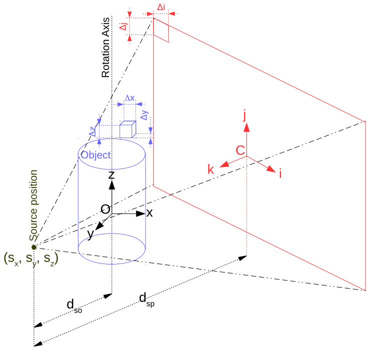

- $(\Delta x, \Delta y, \Delta z)$: voxel dimension;
- $(\Delta i, \Delta j)$: projection pixel dimension;
- (s_x, s_y, s_z): source position for projection θ;
- (c_x, c_y, c_z): panel center position of projection θ;
- d_{SO}: distance source $S \leftrightarrow$ rotation axis;
- d_{SP}: distance source $S \leftrightarrow$ panel center C;
- pitch: Z-translation (helical scanning);
- panel curvature;
- $W \times H \times D$: reconstructed volume size (in voxels);
- $I \times J$: panel size (in pixels);
- ...

- Compute weighting factors w_{ij}:
  - to project each volume voxel into projection pixel (forward process);
  - to back-project residual projection pixels into the volume (backward process).
- Not trivial for fan-beam / cone-beam geometries;

Acquisition properties

How to define the acquisition geometry (matrix A)

X-Ray CT scanner geometry: ray-tracing approach

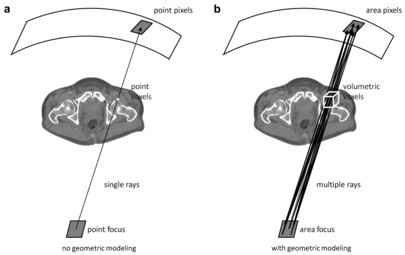

Images from: **Physica medica, 28(2), 94-108 (2012)**.

- Single point approach: continuous case (a);
- Multi-point approach: account for voxel dimension (b):
  - $w_{ij} \propto$ distance crossed by b_i in voxel j;
  - account for spot-source instead of point-source;
  - implies multiple random ray-tracing into the voxel.

Acquisition properties

How to define the acquisition geometry (matrix A)

X-Ray CT scanner geometry: ray-tracing approach

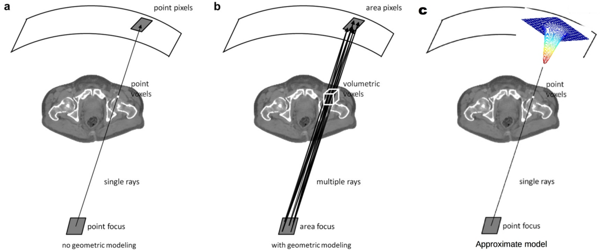

Images from: **Physica medica, 28(2), 94-108 (2012)**.

- Single point approach: continuous case (a);
- Multi-point approach: account for voxel dimension (b):
  - $w_{ij} \propto$ distance crossed by b_i in voxel j;
  - account for spot-source instead of point-source;
  - implies multiple random ray-tracing into the voxel.
- (c) Approximate voxel distribution into projection by Gaussian spreading $\propto \frac{d_{SO}}{d_{SP}}$.

Acquisition properties

How to define the acquisition geometry (matrix A)

X-Ray CT scanner geometry: voxel-shadow projection approach

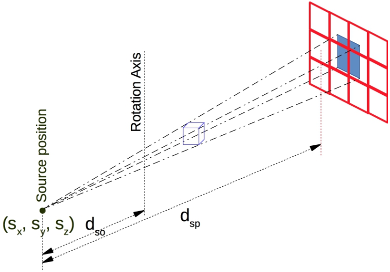

rectangle approximation.

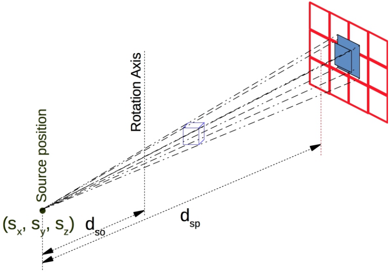

full trapeze.

- project voxel corners from (x, y) plane to get H-trapeze;
- project voxel corners from z-axis to get V-trapeze;
- $H \times V$ and weighting by common area with pixel;
- weighting by ϕ angle to account for angular spreading.

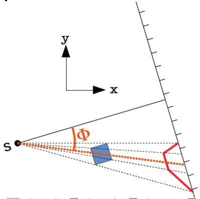

Acquisition properties

How to define the acquisition geometry (matrix A)

X-Ray CT scanner geometry: voxel-shadow projection approach

For each voxel $V(x, y, z)$, **get** $\{p(X, Y, Z) = (x \pm \Delta_X, y \pm \Delta_Y, z \pm \Delta_Z)\}$. **Then, for each** $p(X, Y, Z)$:

$$\begin{aligned}
\rho_1 &= X \sin\theta + Y \cos\theta \\
\rho_2 &= X \cos\theta + Y \sin\theta \\
i_p &= \frac{\rho_1}{d_{SO} + \rho_2} \frac{d_{SP}}{\Delta_i} \\
j_p &= \frac{d_{SP}(Z - s_Z)}{d_{SO} + \rho_2}
\end{aligned}$$

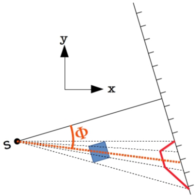

From $\{P_p = (i_p, j_p) \in$ **Panel** $\}$:

- **sort** i_p**'s and create horizontal trapeze** H;
- **sort** j_p**'s and create vertical trapeze** V;
- **compute horizontal angular distorsion**:

$$\begin{aligned}
\phi_H &= \tan^{-1} \frac{|\rho_1|}{d_{SO} + \rho_2} \\
Base_H &= \frac{1}{\max\{\cos|\phi_H|, \sin|\phi_H|\}}
\end{aligned}$$

- **compute vertical angular distorsion**:

$$\begin{aligned}
\phi_V &= \tan^{-1} \frac{Z - s_Z}{d_{SO} + \rho_2} \\
Base_V &= \frac{1}{\max\{\cos|\phi_V|, \sin|\phi_V|\}}
\end{aligned}$$

- **compute acquisition geometry dependent weighing coefficient**:

$$w_{pv} = H \times V \times Base_H \times Base_V$$

Acquisition properties

How to define the acquisition geometry (matrix A)

X-Ray CT scanner geometry: voxel-shadow projection approach

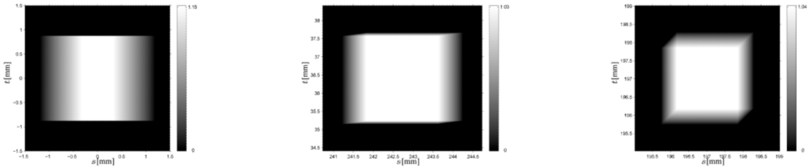

Images from: **Medical Imaging, IEEE Transactions on, 29(11), 1839-1850 (2010)**.

Voxel-shadow approach VS ray-tracing

- Just deal with geometry to get exact representation of the voxel in projection;
- Avoid *simulation approach* of ray-tracing and computation of ray-line and voxel intersection;
- Avoid several reconstruction artefacts (aliasing) due to sampling / discretisation;
- Duality of backward / forward processing;

Acquisition properties

How to define the acquisition geometry (matrix A)

X-Ray CT scanner geometry: voxel-shadow projection approach

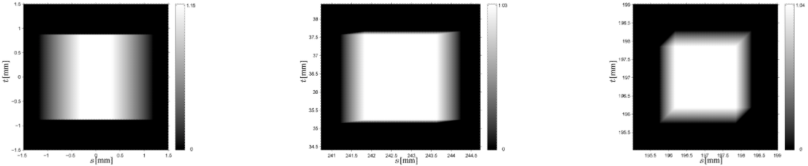

Images from: Medical Imaging, IEEE Transactions on, 29(11), 1839-1850 (2010).

Voxel-shadow approach VS ray-tracing

- Just deal with geometry to get exact representation of the voxel in projection;
- Avoid *simulation approach* of ray-tracing and computation of ray-line and voxel intersection;
- Avoid several reconstruction artefacts (aliasing) due to sampling / discretisation;
- Duality of backward / forward processing;
- For all voxels: until 8 projected points, 2 trapeze functions, 2 distorsions bases to compute;
- Twice per iteration for each projection (forward / backward processing) ... JUST TO GET w_{ij} !!!

Acquisition properties

How to define the acquisition geometry (matrix A)

X-Ray CT scanner geometry: voxel-shadow projection approach

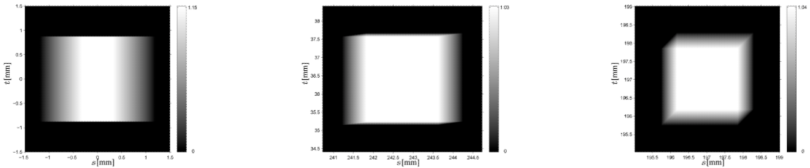

Images from: Medical Imaging, IEEE Transactions on, 29(11), 1839-1850 (2010).

Voxel-shadow approach VS ray-tracing

- Just deal with geometry to get exact representation of the voxel in projection;
- Avoid *simulation approach* of ray-tracing and computation of ray-line and voxel intersection;
- Avoid several reconstruction artefacts (aliasing) due to sampling / discretisation;
- Duality of backward / forward processing;
- For all voxels: until 8 projected points, 2 trapeze functions, 2 distorsions bases to compute;
- Twice per iteration for each projection (forward / backward processing) ... JUST TO GET w_{ij} !!!

Determining $A\{w_{ij}\}$ is the main computational challenge!

Acquisition properties

How to define the acquisition geometry (matrix A)

PET geometry

2D acquisition mode

- low count rate;
- high precision.

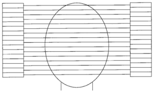

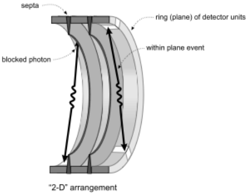

eq. 2D //-beam → by rebinning.

Acquisition properties

How to define the acquisition geometry (matrix A)

PET geometry

2D acquisition mode

- low count rate;
- high precision.

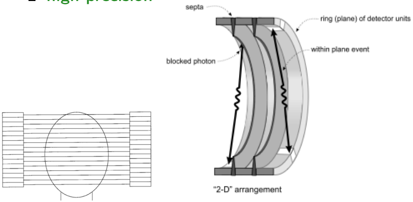

eq. 2D //-beam → by rebinning.

3D acquisition mode

- high count rate;
- time consuming reconstructions and correction of scatter events and noise;

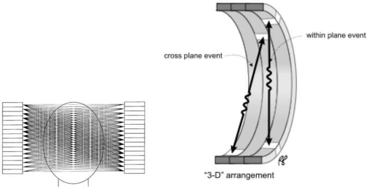

Fully 3D reconstructions should be preferred to rebinning into oblique 2D sinograms.

Acquisition properties

How to define the acquisition geometry (matrix A)

PET geometry

2D acquisition mode

- low count rate;
- high precision·

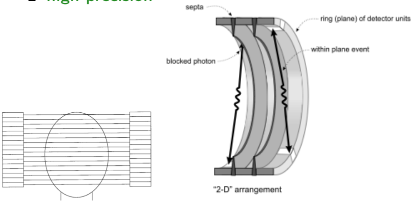

eq. 2D //-beam → by rebinning.

3D acquisition mode

- high count rate;
- time consuming reconstructions and correction of scatter events and noise;

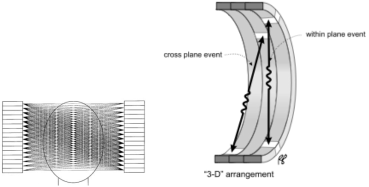

Fully 3D reconstructions should be preferred to rebinning into oblique 2D sinograms.

Direct 3D reconstructions imply:

- each sensor views a cone beam proportional to depth;
- can be viewed as complementary of X-Ray geometries;
- Iterative reconstructions only, using similar ray-tracing / voxel shadow approaches.

Acquisition properties

How to define the acquisition geometry (matrix A)

PET geometry + IR

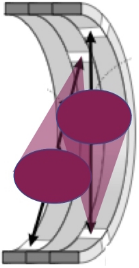

Determining coefficients w_{ij}:

- **Scanner geometry must be known**;
- **Sensor / collimation properties (cone view)**;

Acquisition properties

How to define the acquisition geometry (matrix A)

PET geometry + IR

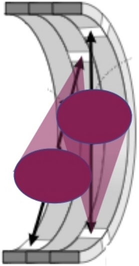

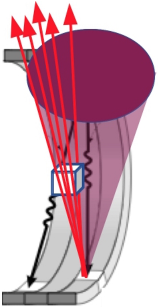

Determining coefficients w_{ij}:

- **Scanner geometry must be known;**
- **Sensor / collimation properties (cone view);**

Ray-tracing approach:

- **Random ray-line from voxel to sensors (all directions) + selection on sensors a.t. collimators (simulation);**
- **Random ray-line from sensor to voxel (restricted to viewing-cone) + intersection voxel/line;**

Acquisition properties

How to define the acquisition geometry (matrix A)

PET geometry + IR

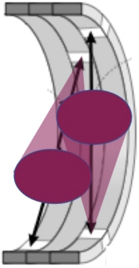

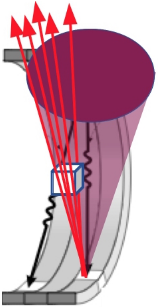

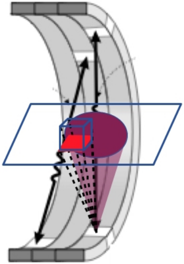

Determining coefficients w_{ij}:

- Scanner geometry must be known;
- Sensor / collimation properties (cone view);

Ray-tracing approach:

- Random ray-line from voxel to sensors (all directions) + selection on sensors a.t. collimators (simulation);
- Random ray-line from sensor to voxel (restricted to viewing-cone) + intersection voxel/line;

Voxel-shadow approach:

- plane normal to the sensor normal and voxel center;
- project viewing cone base on the plane;
- project voxel edges on the plane (get voxel-shadow);
- intersection between cone-base and voxel-shadow;

Acquisition properties

How to define the acquisition geometry (matrix A)

PET geometry + IR

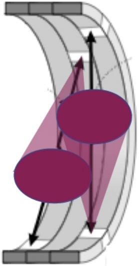

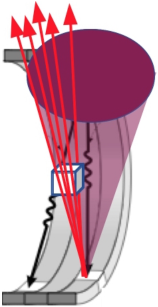

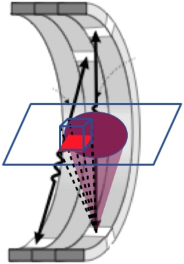

Determining coefficients w_{ij}:

- **Scanner geometry must be known;**
- **Sensor / collimation properties (cone view);**

Ray-tracing approach:

- **Random ray-line from voxel to sensors (all directions) + selection on sensors a.t. collimators (simulation);**
- **Random ray-line from sensor to voxel (restricted to viewing-cone) + intersection voxel/line;**

Voxel-shadow approach:

- **plane normal to the sensor normal and voxel center;**
- **project viewing cone base on the plane;**
- **project voxel edges on the plane (get voxel-shadow);**
- **intersection between cone-base and voxel-shadow;**

Time consuming computation of $R\{w_{ij}\}$!

- How to define the projection matrix A (acquisition geometry);
- Forward model including appropriate physics of radiation;
- Incorporate *a priori* on solution / noise distribution, motion correction, ...

definition of SPECT forward model ?

$$R_i = \sum_j w_{ij} \lambda_j \Leftrightarrow R = A\lambda$$

Acquisition properties

Forward model including appropriate physics of radiation

definition of SPECT forward model ?

$$R_i = \sum_j w_{ij} \lambda_j \Leftrightarrow R = A\lambda$$

Towards accurate definition of SPECT forward-model

$$R_i = \sum w_{ij} p_j \omega_j(E_{ph}) \mu_{j \to i} \lambda_j \Leftrightarrow R = \mathrm{A} \times \mathrm{P} \times \Omega \times M\lambda$$

- $A\{w_{ij}\}$: acquisition geometry weighting coefficient between sensor i and voxel j;
- $P\{p_j\}$: point spread function of the sensor (due to septal penetration);
- $\Omega\{\omega_j(E_{ph})\}$: response or windowing on sensor j to the energy E of counted photon ph;
- $M\{\mu_{j \to i}\}$: attenuation encountered by photons emitted in j along the line from j to i;
- ...

Acquisition properties

Forward model including appropriate physics of radiation

- $A\{w_{ij}\}$: acquisition geometry weighting coefficient between sensor i and voxel j;

Acquisition properties

Forward model including appropriate physics of radiation

- $A\{w_{ij}\}$: acquisition geometry weighting coefficient between sensor i and voxel j;
- $P\{p_j\}$: point spread function of the sensor (due to septal penetration);

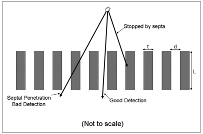

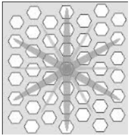
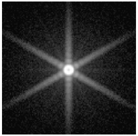

- **Thicker collimator septa but sensitivity loss (implying higher dose delivered)**;
- **PSF deconvolution into projection prior to CT reconstruction**;

Acquisition properties

Forward model including appropriate physics of radiation

- $A\{w_{ij}\}$: acquisition geometry weighting coefficient between sensor i and voxel j;
- $P\{p_j\}$: point spread function of the sensor (due to septal penetration);

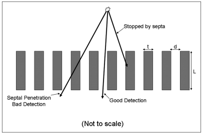

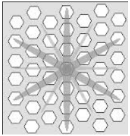

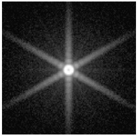

- **Thicker collimator septa but sensitivity loss (implying higher dose delivered)**;
- **PSF deconvolution into projection prior to CT reconstruction**;
- Accurate in IR (convolve forward-projector instead of deconvolve back-projection).

Acquisition properties

Forward model including appropriate physics of radiation

- $A\{w_{ij}\}$: acquisition geometry weighting coefficient between sensor i and voxel j;
- $P\{p_j\}$: point spread function of the sensor (due to septal penetration);

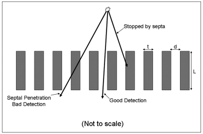

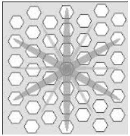
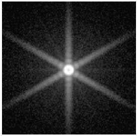

  - **Thicker collimator septa but sensitivity loss (implying higher dose delivered)**;
  - **PSF deconvolution into projection prior to CT reconstruction**;
  - Accurate in IR (convolve forward-projector instead of deconvolve back-projection).
- $\Omega\{\omega_j(E_{ph})\}$: response or windowing on sensor j to the energy E of counted photon ph;

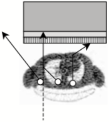
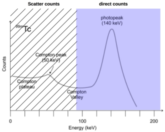

  - **Hardware windowing ? Software windowing ? Pre-processing into projections ?**

Acquisition properties

Forward model including appropriate physics of radiation

- $A\{w_{ij}\}$: acquisition geometry weighting coefficient between sensor i and voxel j;
- $P\{p_j\}$: point spread function of the sensor (due to septal penetration);

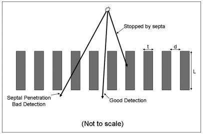

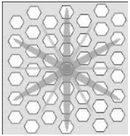

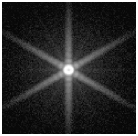

  - **Thicker collimator septa but sensitivity loss (implying higher dose delivered)**;
  - **PSF deconvolution into projection prior to CT reconstruction**;
  - Accurate in IR (convolve forward-projector instead of deconvolve back-projection).
- $\Omega\{\omega_j(E_{ph})\}$: response or windowing on sensor j to the energy E of counted photon ph;

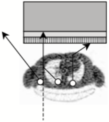

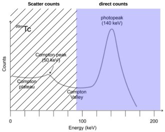

  - **Hardware windowing ? Software windowing ? Pre-processing into projections ?**
  - Software windowing if modelled in the forward-projection of an IR (xSPECT).

Acquisition properties

Forward model including appropriate physics of radiation

- $A\{w_{ij}\}$: acquisition geometry weighting coefficient between sensor i and voxel j;
- $P\{p_j\}$: point spread function of the sensor (due to septal penetration);

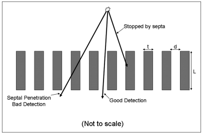

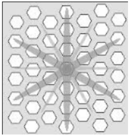

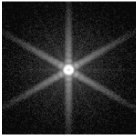

  - **Thicker collimator septa but sensitivity loss (implying higher dose delivered)**;
  - **PSF deconvolution into projection prior to CT reconstruction**;
  - Accurate in IR (convolve forward-projector instead of deconvolve back-projection).
- $\Omega\{\omega_j(E_{ph})\}$: response or windowing on sensor j to the energy E of counted photon ph;

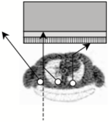

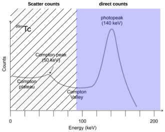

  - **Hardware windowing ? Software windowing ? Pre-processing into projections ?**
  - Software windowing if modelled in the forward-projection of an IR (xSPECT).
- $M\{\mu_{j\rightarrow i}\}$: attenuation encountered by photons emitted in j along the line from j to i;
  - **By using X-Ray CT scan as attenuation map** (hard to achieve as pre-processing);

Acquisition properties

Forward model including appropriate physics of radiation

- $A\{w_{ij}\}$: acquisition geometry weighting coefficient between sensor i and voxel j;
- $P\{p_j\}$: point spread function of the sensor (due to septal penetration);

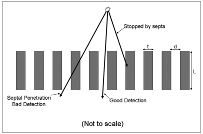

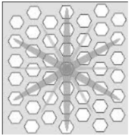
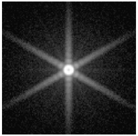

  - **Thicker collimator septa but sensitivity loss (implying higher dose delivered)**;
  - **PSF deconvolution into projection prior to CT reconstruction**;
  - Accurate in IR (convolve forward-projector instead of deconvolve back-projection).
- $\Omega\{\omega_j(E_{ph})\}$: response or windowing on sensor j to the energy E of counted photon ph;

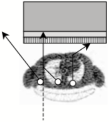
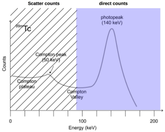

  - **Hardware windowing ? Software windowing ? Pre-processing into projections ?**
  - Software windowing if modelled in the forward-projection of an IR (xSPECT).
- $M\{\mu_{j\rightarrow i}\}$: attenuation encountered by photons emitted in j along the line from j to i;
  - **By using X-Ray CT scan as attenuation map (hard to achieve as pre-processing)**;
  - Straightforward when using IR.

Acquisition properties

Forward model including appropriate physics of radiation

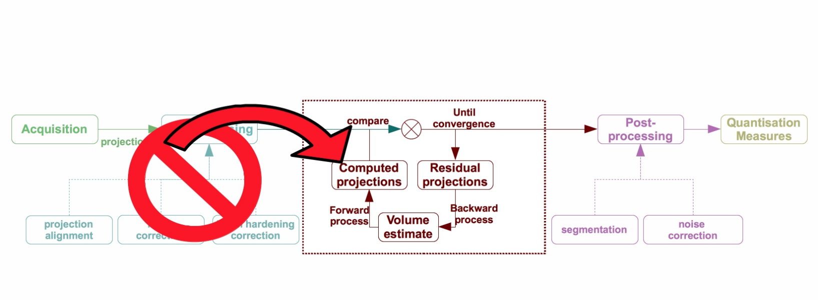

Reminder

Reduce number of sequential processing that increase and transmit errors / approximations to sub-sequent treatments by including everything into the forward-projection of the iterative reconstruction:

- All processing performed at once;
- Backward-checking inducing by the IR.

SPECT forward-model

$$R_i = \sum \underbrace{w_{ij} p_j \omega_j (E_{ph}) \mu_{j \to i}}_{h_{ij}} \lambda_j \Leftrightarrow R = H\lambda$$

where:

- h_{ij} is the probability that pixel j counts photons emitted from i.
- Similar model for PET imaging (H also includes LOR correlations).

SPECT forward-model

$$R_i = \sum \underbrace{w_{ij} p_j \omega_j (E_{ph}) \mu_{j \to i}}_{h_{ij}} \lambda_j \Leftrightarrow R = H\lambda$$

where:

- h_{ij} is the probability that pixel j counts photons emitted from i.
- Similar model for PET imaging (H also includes LOR correlations).

And now ? How to reconstruct λ ?

- Algebraic techniques:
  - include the acquisition geometry / discretisation;

SPECT forward-model

$$R_i = \sum \underbrace{w_{ij} p_j \omega_j (E_{ph}) \mu_{j \to i}}_{h_{ij}} \lambda_j \Leftrightarrow R = H\lambda$$

where:

- h_{ij} is the probability that pixel j counts photons emitted from i.
- Similar model for PET imaging (H also includes LOR correlations).

And now ? How to reconstruct λ ?

- Algebraic techniques:
  - include the acquisition geometry / discretisation;
- Statistical methods:
  - include the acquisition geometry / discretisation;
  - based on a statistical noise model;
  - can include a *a priori* on the solution (bayesian).

Outline

Introduction to tomography

- **Processing sequence;**
- **Computed tomography.**

Introduction to Iterative Reconstruction

- **Examples;**
- **Algebraic reconstruction technique (ART);**
- **Convergence.**

From definitions of acquisition properties ...

- **Projection matrix;**
- **Forward model;**
- **A priori on solution.**

... to statistical methods

- **for emission tomography;**
- **for transmission tomography.**

Towards application based optimisations

- **Some examples;**
- **Concept of full iterative techniques (co-design).**

Noise model of the acquisition represented as a Poisson distribution:

$$R_i \approx Poisson\left\{\sum_j h_{ij}\lambda_j\right\}$$

Is valid since:

- Number of atoms of the biomarker follows a Poisson distribution;
- Spatial localisations of biomarkers are independent;
- Detection of emitted particules are independent processus.

Noise model of the acquisition represented as a Poisson distribution:

$$R_i \approx Poisson\left\{\sum_j h_{ij}\lambda_j\right\}$$

Is valid since:

- Number of atoms of the biomarker follows a Poisson distribution;
- Spatial localisations of biomarkers are independent;
- Detection of emitted particules are independent processus.

$\Rightarrow$ Pre-processing to correct attenuation, PSF, energy windowing leads to non-Poisson projections !

Noise model of the acquisition represented as a Poisson distribution:

$$R_i \approx Poisson\left\{\sum_j h_{ij}\lambda_j\right\}$$

Is valid since:

- Number of atoms of the biomarker follows a Poisson distribution;
- Spatial localisations of biomarkers are independent;
- Detection of emitted particules are independent processus.

$\Rightarrow$ Pre-processing to correct attenuation, PSF, energy windowing leads to non-Poisson projections !

$\Rightarrow$ Everything has to be include in the matrix H of the forward model.

Statistical methods

Expectation Maximisation (EM)

$$p(R|\lambda) = \prod_i \frac{\mathrm{e}^{-\sum_j h_{ij}\lambda_j} (\sum_j h_{ij}\lambda_j)^{R_i}}{R_i!}$$

$$p(R|\lambda) = \prod_i \frac{\mathrm{e}^{-\sum_j h_{ij}\lambda_j} (\sum_j h_{ij}\lambda_j)^{R_i}}{R_i!}$$

Maximising probability $p(R|\lambda) = p(\lambda|R)$ without a priori on λ ($p(\lambda) = 1$)

$\Leftrightarrow$ **maximisation the log-likelihood**:

$$L = \log p(R|\lambda) = \sum_i R_i \log(\sum_j h_{ij}\lambda_j) - \sum_j h_{ij}\lambda_j - \log R_i!$$

Statistical methods

Expectation Maximisation (EM)

$$p(R|\lambda) = \prod_i \frac{e^{-\sum_j h_{ij}\lambda_j}(\sum_j h_{ij}\lambda_j)^{R_i}}{R_i!}$$

Maximising probability $p(R|\lambda) = p(\lambda|R)$ without a priori on λ $(p(\lambda) = 1)$

$\Leftrightarrow$ maximisation the log-likelihood:

$$L = \log p(R|\lambda) = \sum_i R_i \log(\sum_j h_{ij}\lambda_j) - \sum_j h_{ij}\lambda_j - \log R_i!$$

$\Leftrightarrow$ minimising $\partial_\lambda L = \sum_i R_i \frac{\sum_j h_{ij}}{\sum_j h_{ij}\lambda_j} - \sum_j h_{ij} = 0 \Leftrightarrow \sum_i \sum_j h_{ij} = \sum_i R_i \frac{\sum_j h_{ij}}{\sum_j h_{ij}\lambda_j}$

Independent for each voxel j: $\Leftrightarrow 1 = \frac{1}{\sum_i h_{ij}} \sum_i h_{ij} \frac{R_i}{\sum_j h_{ij}\lambda_j}$

Statistical methods

Expectation Maximisation (EM)

$$p(R|\lambda) = \prod_i \frac{e^{-\sum_j h_{ij}\lambda_j}(\sum_j h_{ij}\lambda_j)^{R_i}}{R_i!}$$

Maximising probability $p(R|\lambda) = p(\lambda|R)$ without a priori on λ $(p(\lambda) = 1)$

$\Leftrightarrow$ maximisation the log-likelihood:

$$L = \log p(R|\lambda) = \sum_i R_i \log(\sum_j h_{ij}\lambda_j) - \sum_j h_{ij}\lambda_j - \log R_i!$$

$\Leftrightarrow$ minimising $\partial_\lambda L = \sum_i R_i \frac{\sum_j h_{ij}}{\sum_j h_{ij}\lambda_j} - \sum_j h_{ij} = 0 \Leftrightarrow \sum_i \sum_j h_{ij} = \sum_i R_i \frac{\sum_j h_{ij}}{\sum_j h_{ij}\lambda_j}$

Independent for each voxel j: $\Leftrightarrow 1 = \frac{1}{\sum_i h_{ij}} \sum_i h_{ij} \frac{R_i}{\sum_j h_{ij}\lambda_j}$

MLEM algorithm update:

$$\lambda_j^{k+1} = \frac{\lambda_j^k}{\sum_i h_{ij}} \sum_i h_{ij} \frac{R_i}{\underbrace{\sum_j h_{ij}\lambda_j^k}_{\hat{R}_i^k}}$$

where:

- R_i: acquired projection line i
- $\hat{R}_i^k = \sum_j h_{ij}\lambda_j^k$: projection line computed from previous estimate λ^k

Statistical methods

Maximum a Posteriori (MAP-) Expectation Maximisation (EM)

Main goal

- WHY? If the update step sounds inadequate (erronous), detect, reduce or avoid it;
- HOW? By adding a priori on the solution ($p(\lambda) \neq 1$) that preserves locally defined characteristics.

Main goal

- WHY? If the update step sounds inadequate (erronous), detect, reduce or avoid it;
- HOW? By adding a priori on the solution ($p(\lambda) \neq 1$) that preserves locally defined characteristics.

$\Leftrightarrow$ Maximisation of $p(R|\lambda)p(\lambda)$

- Define a local a priori on the solution linking neighbourhood voxels (Gibbs prior):

$$p(\lambda) = e^{-\sum_j \underbrace{\sum_{k \in \mathcal{N}(j)} y_{jk} \Phi(\lambda(j) - \lambda(k))}_{\text{Markov field}}} \quad \text{where} \begin{cases} \mathcal{N}(j)\text{: neighbourhood of pixel } j, \\ \Phi(\cdot)\text{: potential function}, \\ y_{jk}\text{: weight factor}. \end{cases} \tag{8}$$

Main goal

- WHY? If the update step sounds inadequate (erronous), detect, reduce or avoid it;
- HOW? By adding a priori on the solution ($p(\lambda) \neq 1$) that preserves locally defined characteristics.

$\Leftrightarrow$ Maximisation of $p(R|\lambda)p(\lambda)$

- Define a local a priori on the solution linking neighbourhood voxels (Gibbs prior):

$$p(\lambda) = e^{-\sum_j \underbrace{\sum_{k \in \mathcal{N}(j)} y_{jk} \Phi(\lambda(j) - \lambda(k))}_{\text{Markov field}}} \quad \text{where} \begin{cases} \mathcal{N}(j)\text{: neighbourhood of pixel } j, \\ \Phi(\cdot)\text{: potential function,} \\ y_{jk}\text{: weight factor.} \end{cases} \tag{8}$$

- Use appropriate potential function:
  - Wiener / Hunt: $\Phi(x) = \alpha x^2$;
  - Geman / McClure: $\Phi(x) = \alpha * t^2 * (\frac{x}{t})^2 / (1 + (\frac{x}{t})^2)$;
  - Hebert / Leahy: $\Phi(x) = \alpha t^2 \log(1 + (\frac{x}{t})^2)$;
  - L1/L2 LogCosH: $\Phi(x) = 2t \log cosh \frac{|x|}{t}$;
  - Huber, Hyperbolique, Fair function, ...

Statistical methods

Maximum a Posteriori (MAP-) Expectation Maximisation (EM)

MAP-EM update:

$$\lambda_j^{k+1} = \frac{\lambda_j^k}{\sum_i h_{ij} + \sum_{k \in \mathcal{N}(j)} y_{jk} \Phi^{'}(\lambda_j - \lambda_k)} \sum_i h_{ij} \frac{R_i}{\hat{R}_i^k}$$

Statistical methods

Maximum a Posteriori (MAP-) Expectation Maximisation (EM)

MAP-EM update:

$$\lambda_j^{k+1} = \frac{\lambda_j^k}{\sum_i h_{ij} + \sum_{k \in \mathcal{N}(j)} y_{jk} \Phi^{'}(\lambda_j - \lambda_k)} \sum_i h_{ij} \frac{R_i}{\hat{R}_i^k}$$

Any EM or MAP-EM algorithm can be derived as:

- **Simultaneous (one projection / update): SEM / MAP-SEM;**
- **Ordered subsets: OSEM, MAP-OSEM, RAMLA (one projection-line / update);**

Statistical methods

Maximum a Posteriori (MAP-) Expectation Maximisation (EM)

MAP-EM update:

$$\lambda_j^{k+\mathbf{1}} = \frac{\lambda_j^k}{\sum_i h_{ij} + \sum_{k \in \mathcal{N}(j)} y_{jk} \Phi'(\lambda_j - \lambda_k)} \sum_i h_{ij} \frac{R_i}{\hat{R}_i^k}$$

Any EM or MAP-EM algorithm can be derived as:

- Simultaneous (one projection / update): SEM / MAP-SEM;
- Ordered subsets: OSEM, MAP-OSEM, RAMLA (one projection-line / update);
- Flash3D = OSEM

Statistical methods

Maximum a Posteriori (MAP-) Expectation Maximisation (EM)

MAP-EM update:

$$\lambda_j^{k+1} = \frac{\lambda_j^k}{\sum_i h_{ij} + \sum_{k \in \mathcal{N}(j)} y_{jk} \Phi^{'}(\lambda_j - \lambda_k)} \sum_i h_{ij} \frac{R_i}{\hat{R}_i^k}$$

Any EM or MAP-EM algorithm can be derived as:

- Simultaneous (one projection / update): SEM / MAP-SEM;
- Ordered subsets: OSEM, MAP-OSEM, RAMLA (one projection-line / update);
- Flash3D = OSEM

Remarks

- Poisson VS Gaussian: update steps similar than ART;
- other implementations: Conjugate Gradient (CG);

Statistical methods

Maximum a Posteriori (MAP-) Expectation Maximisation (EM)

MAP-EM update:

$$\lambda_j^{k+1} = \frac{\lambda_j^k}{\sum_i h_{ij} + \sum_{k \in \mathcal{N}(j)} y_{jk} \Phi^{'}(\lambda_j - \lambda_k)} \sum_i h_{ij} \frac{R_i}{\hat{R}_i^k}$$

Any EM or MAP-EM algorithm can be derived as:

- Simultaneous (one projection / update): SEM / MAP-SEM;
- Ordered subsets: OSEM, MAP-OSEM, RAMLA (one projection-line / update);
- Flash3D = OSEM

Remarks

- Poisson VS Gaussian: update steps similar than ART;
- other implementations: Conjugate Gradient (CG);
- xSPECT = OS-CG

Acquisition properties

- How to define the projection matrix A (acquisition geometry);
- Forward model including appropriate physics of radiation;
- Incorporate *a priori* on solution / noise distribution, motion correction, ...

Convergence

- What the better first estimate ?;
- Ordered subsets of projections;
- How to detect it and avoid divergence;

Acquisition properties

- How to define the projection matrix A (acquisition geometry);
- Forward model including appropriate physics of radiation;
- Incorporate *a priori* on solution / noise distribution, motion correction, ...

Convergence

- What the better first estimate ?;
- Ordered subsets of projections;
- How to detect it and avoid divergence;

A priori on the solution leads to MAP methods *regularising* / *penalising* the update.

From transmittance to absorbance

$$R_i = I_i \mathrm{e}^{-\sum_j h_{ij}\mu_j} \Leftrightarrow A_i = \log \frac{I_i}{R_i} = \sum_j h_{ij}\mu_j$$

$\Rightarrow$ then, algebraic techniques or expectation maximisation algorithms.

From transmittance to absorbance

$$R_i = I_i \mathrm{e}^{-\sum_j h_{ij}\mu_j} \Leftrightarrow A_i = \log \frac{I_i}{R_i} = \sum_j h_{ij}\mu_j$$

$\Rightarrow$ then, algebraic techniques or expectation maximisation algorithms.

Directly from transmittance data

$$R_i = I_i \mathrm{e}^{-\sum_j h_{ij}\mu_j}$$

$\Rightarrow$ then, Newton-Raphson to maximise $L = \log\left[p(R|\mu)p(\mu)\right]$:

$$\mu^t_{s+1}(j) = \mu^t_s(j) - \frac{\partial L}{\partial^2 L}$$

$\Rightarrow$ $\log p(R|\mu)$ and $\log p(\mu)$ twice derivable:

From transmittance to absorbance

$$R_i = I_i \mathrm{e}^{-\sum_j h_{ij}\mu_j} \Leftrightarrow A_i = \log \frac{I_i}{R_i} = \sum_j h_{ij}\mu_j$$

⇒ then, algebraic techniques or expectation maximisation algorithms.

Directly from transmittance data

$$R_i = I_i \mathrm{e}^{-\sum_j h_{ij}\mu_j}$$

⇒ then, Newton-Raphson to maximise $L = \log\left[p(R|\mu)p(\mu)\right]$:

$$\mu_{s+1}^t(j) = \mu_s^t(j) - \frac{\partial L}{\partial^2 L}$$

⇒ $\log p(R|\mu)$ and $\log p(\mu)$ twice derivable:

$$\mu_{s+1}^t(j) = \mu_s^t(j) + \frac{\sum_{i\in S(s)} w_{ij}\left[\hat{R}_s^t(i) - R(i)\right] - \sum_{k\in\mathcal{N}(j)} y_{jk}\Phi'\left[\mu_s^t(j) - \mu_s^t(k)\right]}{\sum_{i\in S(s)} w_{ij}\left(\sum_l w_{il}\right)\hat{R}_s^t(i) + \sum_{k\in\mathcal{N}(j)} y_{jk}\Phi''\left[\mu_s^t(j) - \mu_s^t(k)\right]}$$

⇒ Ordered Subsets Convex (OSC) algorithm:

- Reduce metal artefacts (non-linearity of transmittance VS linearity of absorbance);
- Update μ directly from R and not from intermediate step A.

Outline

Introduction to tomography

- **Processing sequence**;
- **Computed tomography**.

Introduction to Iterative Reconstruction

- **Examples**;
- **Algebraic reconstruction technique (ART)**;
- **Convergence**.

From definitions of acquisition properties ...

- **Projection matrix**;
- **Forward model**;
- **A priori on solution**.

... to statistical methods

- **for emission tomography**;
- **for transmission tomography**.

Towards application based optimisations

- **Some examples**;
- **Concept of full iterative techniques (co-design)**.

Towards application based-optimisations

From single-energy X-Ray CT

- Linear attenuation coefficient, i.e. estimation M (PET/SPECT) from X-Ray-CT:

$$R_i = \sum w_{ij} p_j \omega_j(E_{ph}) \mu_{j \to i} \lambda_j$$

Towards application based-optimisations

From single-energy X-Ray CT

- Linear attenuation coefficient, i.e. estimation M (PET/SPECT) from X-Ray-CT:

$$R_i = \sum w_{ij} p_j \omega_j (E_{ph}) \mu_{j \rightarrow i} \lambda_j$$

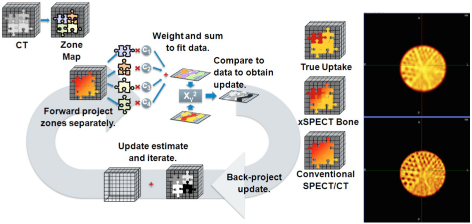

Images from: Vija, H. A. "Introduction to xSPECT technology: evolving multi-modal SPECT to become context-based and quantitative. Siemens Medical Solutions USA." (2014).

Towards application based-optimisations

From single-energy X-Ray CT

- Linear attenuation coefficient, i.e. estimation M (PET/SPECT) from X-Ray-CT:

$$R_i = \sum w_{ij} p_j \omega_j(E_{ph}) \mu_{j \to i} \lambda_j$$

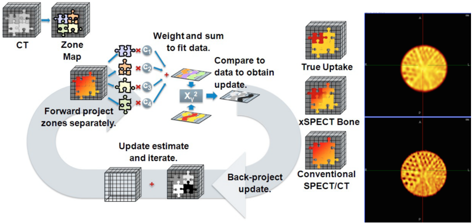

Images from: Vija, H. A. "Introduction to xSPECT technology: evolving multi-modal SPECT to become context-based and quantitative. Siemens Medical Solutions USA." (2014).

$\Rightarrow$ From single-energy acquisition: segmentation by material fitting (dictionary) + re-interpret CT scan at the energy of SPECT / PET rays (xSPECT).

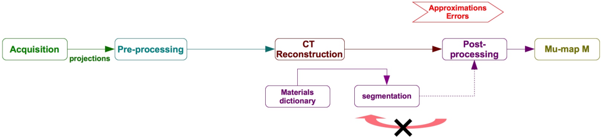

Towards application based-optimisations

From dual / multi-energy X-Ray CT tomography

- "High dynamic range" CT imaging:
  - **By sinogram decomposition (bone / soft tissues): separation from 80 kVp to 100 kVp, and 100 to 130 kVp to directly get 100 kVp sinogram;**
  - **By tomogram combination (material estimation from / to attenuation coefficient curves): reconstruct images μ_{80} and μ_{130} create image at μ_{100} after material labelling from tables.**

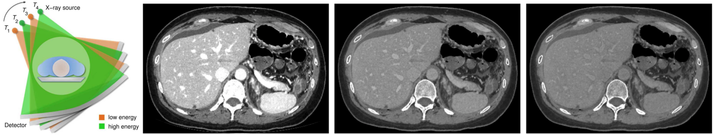

Figure: **Images from IEEE Trans. on Med. Im., Vol. 33, No.1, January 2014: 117-134**

Towards application based-optimisations

From dual / multi-energy X-Ray CT tomography

- "High dynamic range" CT imaging:
  - **By sinogram decomposition (bone / soft tissues): separation from 80 kVp to 100 kVp, and 100 to 130 kVp to directly get 100 kVp sinogram;**
  - **By tomogram combination (material estimation from / to attenuation coefficient curves): reconstruct images μ_{80} and μ_{130} create image at μ_{100} after material labelling from tables.**

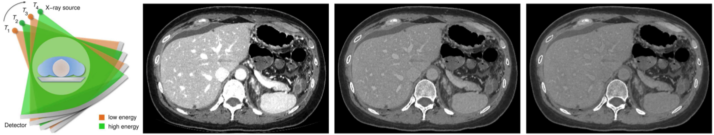

Figure: **Images from IEEE Trans. on Med. Im., Vol. 33, No.1, January 2014: 117-134**

- Remove / highlight specific data (from tomograms):

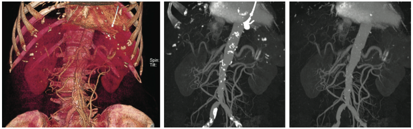

Figure: **Angiography: Tomograms obtained from acquisitions at 80 kVp and 140 kVp: ((a) coronal VR) are combined to remove bones (b) or calcific plaques (c). Images from Diagn. Interv. Radiol. 17.3 (2011): 181-194.**

Towards application based-optimisations

From dual / multi-energy X-Ray CT tomography

- Segmentation by chemical labelling from dual-energy acquisition.

$$\begin{aligned} \mu_E(x) &= \frac{K_\mathbf{1}}{E^k} Z^n(x)\rho(x) + K_\mathbf{2}\mathscr{F}_{KN}(E)\rho(x) \\ &= \underbrace{f^E_{e^-}(Z(x), \rho(x))}_{\textbf{Photoelectric effect}} + \underbrace{f^E_{CS}(\rho(x))}_{\textbf{Compton scattering}} \end{aligned} \tag{9}$$

where $\mathscr{F}_{KN}(E)$: Klein-Nishina function, E: energy, $K1$ and $K2$: two constants determined experimentally.

Towards application based-optimisations

From dual / multi-energy X-Ray CT tomography

- Segmentation by chemical labelling from dual-energy acquisition.

$$\begin{aligned} \mu_E(x) &= \frac{K_1}{E^k} Z^n(x)\rho(x) + K_2 \mathscr{F}_{KN}(E)\rho(x) \\ &= \underbrace{f^E_{e-}(Z(x), \rho(x))}_{\textbf{Photoelectric effect}} + \underbrace{f^E_{CS}(\rho(x))}_{\textbf{Compton scattering}} \end{aligned} \tag{9}$$

where $\mathscr{F}_{KN}(E)$: Klein-Nishina function, E: energy, $K1$ and $K2$: two constants determined experimentally.

$\Rightarrow$ Dual material-labelling and iterative CT reconstruction, with 2 additional inputs:

Material dictionary:

Name	Chemical Formula	ρ (g/cc)	Z_{eff}	
Air	Air	0.001	7.2240	
Iron Pure	Fe	5.600	26.0000	
Rutile	TiO_2	4.200	19.0006	
Siderite	$FeCO_3$	3.960	21.0932	
Na-Montmorillonite	$NaAl_5MgSi_{12}O_{30}(OH)_6$	2.650	11.4620	
Water	H_2O	1.000	7.5195	
Graphite	C	2.300	6.0000	
Calcite	$CaCO_3$	2.710	15.7100	
Dolomite	$CaMg(CO_3)_2$	2.870	13.7438	
Quartz Mineral	SiO_2	2.650	11.5800	
Aluminium Pure	Al	2.700	13.0000	
Anhydrite	$CaSO_4$	2.950	15.6847	
Fused Quartz	SiO_2	2.200	11.7842	
Pyrite	FeS_2	5.020	21.9588	
Barite	$BaSO_4$	4.500	47.2008	
Na-Feldspar	$NaAlSi_3O_8$	2.610	11.5534	
K-Feldspar	$KAlSi_3O_8$	2.530	13.3895	
Kaolinite	$Al_2Si_2O_5(OH)_4$	1.300	11.1622	
Illite	$KAl_3Si_3O_{10}(OH)_2$	2.800	9.6058	
Ca-Montmorillonite	$Ca_{0.5}Al_5MgSi_{12}O_{30}(OH)_6$	2.650	11.8277	
Chlorite	$Fe_2Mg_2Al_2Si_2A_{12}O_{10}(OH)_8$	2.900	11.6449	
Celestite	$SrSO_4$	3.900	30.4686	
Talc	$Mg_3Si_4O_{10}(OH)_2$	2.750	8.4538	
Halite	NaCl	2.350	15.3295	

Table: **Density ρ and atomic number Z_{eff} for common materials.**

Matching function:

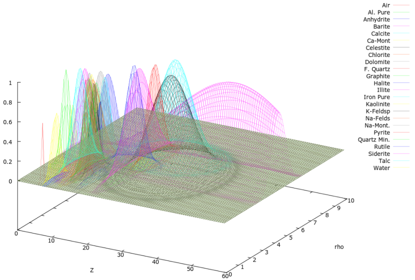

Towards application based-optimisations

From dual / multi-energy X-Ray CT tomography

Calcite	$CaCO_3$	2.710	15.7100	
Quartz Mineral	SiO_2	2.650	11.5800	
Aluminium Pure	Al	2.700	13.0000	
Kaolinite	$Al_2Si_2O_5(OH)_4$	1.300	11.1622	

From dual-energy: hard to achieve except for very different materials:

$$R_i = \int_E I_{E_i} \mathrm{e}^{-\int_x h_{ix} \mu_{E_j} dx} dE$$

$\Rightarrow$ N materials $\Leftrightarrow$ N energy-acquisitions

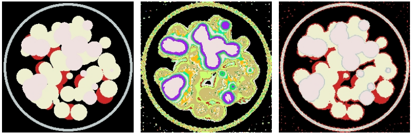

Ref	53.87	87.91
Corr. (in %)	tomogram segmentation	dual mat. labelling / IR

Images from: SPIE Optical Engineering Applications, pp. 921213-921213. International Society for Optics and Photonics, 2014

Towards application based-optimisations

From dual / multi-energy X-Ray CT tomography

Calcite	$CaCO_3$	2.710	15.7100	
Quartz Mineral	SiO_2	2.650	11.5800	
Aluminium Pure	Al	2.700	13.0000	
Kaolinite	$Al_2Si_2O_5(OH)_4$	1.300	11.1622	

From dual-energy: hard to achieve except for very different materials:

$$R_i = \int_E I_{E_i} e^{-\int_x h_{ix} \mu_{E_j} dx} dE$$

$\Rightarrow$ N materials $\Leftrightarrow$ N energy-acquisitions

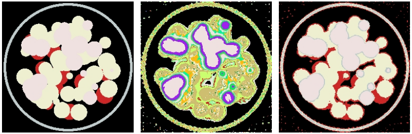

Ref	53.87	87.91
Corr. (in %)	tomogram	dual mat.
	segmentation	labelling / IR

Images from: SPIE Optical Engineering Applications, pp. 921213-921213. International Society for Optics and Photonics, 2014

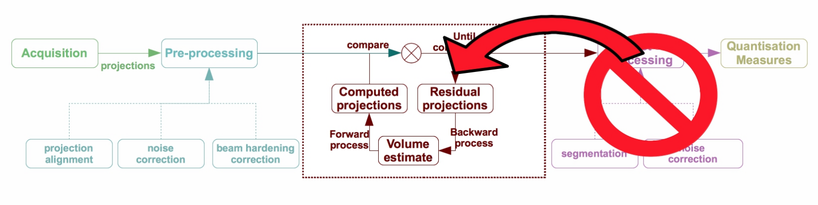

Towards application based-optimisations

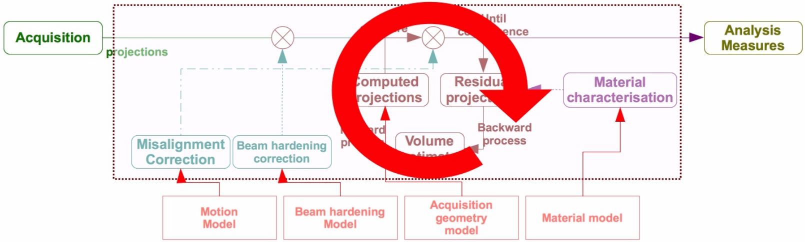

Feedback implicitely performed through the iterations

Towards application based-optimisations

Example: 4D Dynamic tomography with motion-models (cardiac or respiratory phases)

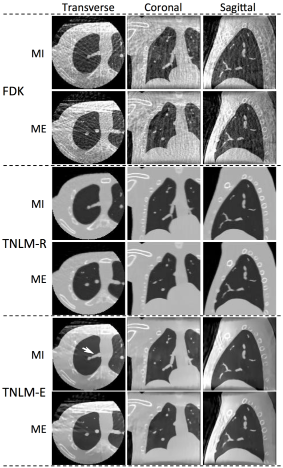

Figure 2. 4D-CBCT images of a NCAT phantom at the MI phase and the ME phase. Top two rows: reconstructed from the FDK algorithm. Middle two rows: reconstructed using our TNLM-R algorithm. Bottom two rows: the FDK results enhanced with our TNLM-E algorithm. The white arrows indicate the tumor-like structure used to compute *CNR*.

Old sequence

- Sort X-Ray projections into multiple respiratory phases (blind or external surrogates);
- Reconstruct each phase with FDK or iterative algorithm (low resolution, deformations).

Towards application based-optimisations

Example: 4D Dynamic tomography with motion-models (cardiac or respiratory phases)

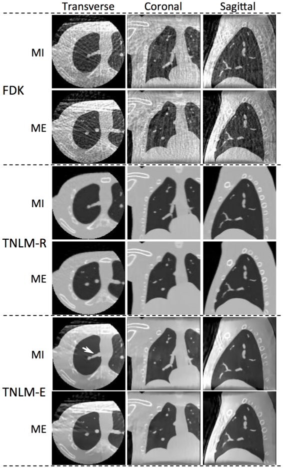

Figure 2. 4D-CBCT images of a NCAT phantom at the MI phase and the ME phase. Top two rows: reconstructed from the FDK algorithm. Middle two rows: reconstructed using our TNLM-R algorithm. Bottom two rows: the FDK results enhanced with our TNLM-E algorithm. The white arrows indicate the tumor-like structure used to compute *CNR*.

Old sequence

- Sort X-Ray projections into multiple respiratory phases (blind or external surrogates);
- Reconstruct each phase with FDK or iterative algorithm (low resolution, deformations).

New sequence

- Define a deformation model into projections / images modelling respiratory phases;
- Iteratively reconstruct each phase from both direct-phase and motion-estimated projections;
- If acquisition data-set: minimising both projection error and motion model with external motion data;
- Elsewhere: minimise motion model equation from images ... not the best solution !

Images from: Jia, Xun, et al. Medical physics 39.9 (2012): 5592-5602. Similar approach for the same purpose in: Schmidt, Mai L., et al. Acta Oncologica 53.8 (2014): 1107-1113 Similar approach cardiac CT in: Tang, Qiulin, et al. Medical physics 39.7 (2012): 4291-4305.

Towards application based-optimisations

Example: 4D Dynamic tomography with motion-models (cardiac or respiratory phases)

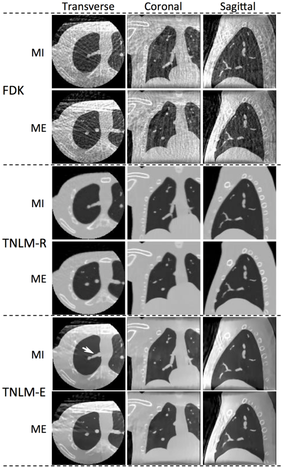

Figure 2. 4D-CBCT images of a NCAT phantom at the MI phase and the ME phase. Top two rows: reconstructed from the FDK algorithm. Middle two rows: reconstructed using our TNLM-R algorithm. Bottom two rows: the FDK results enhanced with our TNLM-E algorithm. The white arrows indicate the tumor-like structure used to compute *CNR*.

Old sequence

- Sort X-Ray projections into multiple respiratory phases (blind or external surrogates);
- Reconstruct each phase with FDK or iterative algorithm (low resolution, deformations).

New sequence

- Define a deformation model into projections / images modelling respiratory phases;
- Iteratively reconstruct each phase from both direct-phase and motion-estimated projections;
- If acquisition data-set: minimising both projection error and motion model with external motion data;
- Elsewhere: minimise motion model equation from images ... not the best solution !

Images from: Jia, Xun, et al. Medical physics 39.9 (2012): 5592-5602. Similar approach for the same purpose in: Schmidt, Mai L., et al. Acta Oncologica 53.8 (2014): 1107-1113 Similar approach cardiac CT in: Tang, Qiulin, et al. Medical physics 39.7 (2012): 4291-4305.

Prediction guided / targeted radiotherapy

Proc. SPIE 9415, Medical Imaging 2015: Image-Guided Procedures, Robotic Interventions, and Modeling, 941510 (March 18, 2015). Martin, James, et al. Physics in medicine and biology 58.6 (2013): 1809.

Conclusion


Dedicated to
Acquisition
Optimized Iterative
CT Reconstruction
Application
« Tune » acquisition

Conclusion

Topical reviews / SoA I.R.:

- Physica Medica 28, 94-108 (2012).
- Brian F. Hutton. Acta Oncologica, 50:6 (2011): 851-858
- Wang, et al. Physics in Medicine and Biology 42.11 (1997): 2215.
- De Pierro, et al. Medical Imaging, IEEE Transactions on 20.4 (2001): 280-288.
- http://www.oralhealthgroup.com/
- Erlandsson, et al. Physics in medicine and biology 57.21 (2012): R119.
- Yan, Ming, et al. Inverse Problems Imaging 7 (2013): 1007-29.
- Nuyts, et al. Physics in medicine and biology 58.12 (2013): R63.
- Erdogan, et al. Physics in medicine and biology 44.11 (1999): 2835.
- Long, Yong, et al. Medical Imaging, IEEE Transactions on 29.11 (2010): 1839-1850.

Optimised / Fully I.R. approaches:

- Jia, Xun, et al. Medical physics 39.9 (2012): 5592-5602.
- Schmidt, et al. Acta Oncologica 53.8 (2014): 1107-1113.
- Tang, Qiulin, et al. Medical physics 39.7 (2012): 4291-4305.
- Proc. SPIE 9415, Medical Imaging 2015: Image-Guided Procedures, Robotic Interventions, and Modeling, 941510 (March 18, 2015).
- Martin, James, et al. Physics in medicine and biology 58.6 (2013): 1809.
- Introduction to xSPECT technology. Siemens Medical Solutions USA." (2014).
- IEEE Trans. on Med. Im., Vol. 33, No.1, January 2014: 117-134.
- Diagn. Interv. Radiol. 17.3 (2011): 181-194.
- SPIE Optical Engineering Applications, pp. 921213-921213 (2014).